

See discussions, stats, and author profiles for this publication at: <https://www.researchgate.net/publication/264975252>

A Novel Solid–Liquid Equilibrium Model for Describing the Adsorption of Associating Asphaltene Molecules onto Solid Surfaces Based on the "Chemical Theory"

ARTICLE *in* ENERGY & FUELS · JULY 2014

Impact Factor: 2.79 · DOI: 10.1021/ef501020d

CITATIONS

6

READS

80

5 AUTHORS, INCLUDING:



Tatiana Montoya

National University of Colombia

6 PUBLICATIONS 25 CITATIONS

SEE PROFILE



Camilo Andres Franco Ariza

National University of Colombia

19 PUBLICATIONS 83 CITATIONS

SEE PROFILE



Nashaat N Nassar

The University of Calgary

65 PUBLICATIONS 885 CITATIONS

SEE PROFILE



Farid B. Cortés

National University of Colombia

83 PUBLICATIONS 226 CITATIONS

SEE PROFILE

A Novel Solid–Liquid Equilibrium Model for Describing the Adsorption of Associating Asphaltene Molecules onto Solid Surfaces Based on the “Chemical Theory”

Tatiana Montoya,[†] Diana Coral,[†] Camilo A. Franco,[†] Nashaat N. Nassar,^{*,‡} and Farid B. Cortés^{*,†}

[†]Grupo de Investigación en Yacimientos de Hidrocarburos, Facultad de Minas, Universidad Nacional de Colombia Sede Medellín, Kra 80 No. 65-223, Medellín, Colombia

[‡]Department of Chemical and Petroleum Engineering, University of Calgary, 2500 University Drive NW, Calgary, Alberta, Canada

S Supporting Information

ABSTRACT: Asphaltenes exhibit an amphiphilic behavior and tend to form colloidal *i*-mers, because of their chemical structure. The formation of colloidal aggregates can generate formation damage for the precipitation and/or deposition of asphaltenes, because of the degree of self-association, altering the wettability of rock surface and significantly affect crude oil viscosity and specific gravity. This study aims at introducing a novel model for describing, at the macroscopic level, the adsorption equilibria of self-associating molecules such as asphaltenes in solution onto solid surfaces based on the “chemical theory”. The model describes the adsorption isotherms temperature-dependent using three parameters, namely, maximum amount adsorbed, constant of *i*-mer reactions, and Henry’s law constant. Furthermore, a temperature-independent model of five parameters, based on the modifications of the constants of reaction and Henry’s law using an Arrhenius-type equation was proposed for estimating the thermodynamics parameters, such as $\Delta G_{\text{ads}}^{\circ}$, $\Delta H_{\text{ads}}^{\circ}$, and $\Delta S_{\text{ads}}^{\circ}$ of the adsorption process. This model improves the understanding of interactions asphaltene–asphaltene and asphaltene–solid surface on the adsorption–equilibrium process. The theoretical predictions of isotherms were validated successfully by determining the root mean-square errors (RSM%) between data obtained from published literature and values predicted for asphaltenes and surfaces with differing chemical natures. More than 40 experimental data taken from literature have been used for validating the solid–liquid equilibrium (SLE) model for describing the adsorption isotherm of asphaltenes from different origins on surfaces with different chemical nature, which shows the model robustness due to the complexity of the liquid phase adsorption for those complex molecules.

1. INTRODUCTION

It is well-known that oil and gas reservoir conditions (i.e., pressure, temperature, and compositions) could vary during the exploitation and production processes of hydrocarbons.¹ Accordingly, the changes of pressure, temperature, and compositions may cause the phenomenon of precipitation of heavy organic solids such as asphaltenes, which decreases the efficiency of the well flow during different stages of production of hydrocarbons.^{1,2} Asphaltene precipitation/deposition is well-known in the oil industry, because it causes many problems, such as reduced permeability and wettability changes in rock appear more frequently in light oils that contain lower amounts of asphaltenes found in deposits whose pressures are higher than the bubble point.² The pressure and temperature are considered as key variables that affect the stability and aggregation behavior of asphaltenes in the reservoir. The viscosity of heavy and extra-heavy oils can dramatically increase,^{3–5} because of the increase in the rate of asphaltene aggregation.^{6–8} Asphaltenes are defined as the heaviest fraction of crude oil that is insoluble in low-molecular-weight paraffins such as *n*-heptane or *n*-pentane, while being soluble in light aromatic hydrocarbons such as toluene, pyridine, or benzene.^{6,8} This definition, based on solubility characteristics, indicates a procedure to isolate asphaltenes from crude oils or bituminous materials, but it does not provide insight into their chemical structure.⁹ In fact, asphaltenes are not a chemical family per se,

and may contain a large heterogeneity of chemical functionalities, which does not provide a complete definition of their molecular properties.^{6,10} However, it is widely accepted that the chemical structure of asphaltenes is generally based on one polycyclic aromatic hydrocarbon (PAH) or many cross-linked PAHs, forming island and archipelago architectures, respectively.^{11–14}

It is important to know that the formation of these structures depends on the asphaltenes source as asphaltene structure could have different components such as heteroatoms, polar and/or nonpolar compounds, H/C ratios, and so forth. Hence, the internal interactions between these components will contribute to the formation of one of the structures mentioned previously.¹⁵ Asphaltenes also contain nonmetallic heteroatoms, such as nitrogen, oxygen, and sulfur, as well as metals, including vanadium, iron, and nickel.^{6,10} Because of its amphiphilic behavior, this structure facilitates asphaltene nucleation and growth and the subsequent formation of colloidal nanoaggregates. Normally, asphaltenes are present in crude oil as colloidal suspensions surrounded by resins in micelle form.¹⁶ The resins do not allow the contact between asphaltene molecules when the system is in equilibrium,

Received: May 5, 2014

Revised: July 18, 2014

Published: July 20, 2014



because the repulsion forces are higher than the van der Waals forces (attraction forces).^{17,18} However, the injection of ionized solvents such as *n*-pentane or toluene can change the concentration of resins, and hence results in having some parts of the asphaltene molecules without resin that causes interactions between asphaltene molecules and subsequent aggregation formation.^{16,18} This is a typical behavior of the commonly known amphiphilic molecules due to their lipophilic and hydrophilic parts.^{19,20} This amphiphilic behavior in the asphaltenes is believed to be due to the presence of the polar molecules, nonpolar molecules, and functional groups with heteroatoms in the asphaltene structure, such as thiophenic, sulfidic, sulfoxide, pyrrolic, pyridine, quinolone, hydroxyl, carbonyl, and carboxyl.^{21,22}

Pernyeszi et al.²³ found that the adsorption of *n*C₇-asphaltenes from mineral oil in several hydrophilic clays minerals is initially due to the interaction between polar parts of asphaltenes and polar parts of the surface resulting in a hydrophobic shell of asphaltenes. Hence, the adsorption of a second layer of asphaltenes over this hydrophobic shell can result in a layer that is more hydrophilic, because of the buildup of outward-facing polar functional groups.^{22,24} Removing asphaltenes from a heavy-oil matrix will result in improving oil quality and enhancing its mobility with less environmental impact.³ Because of its simplicity and applicability at the industrial scale, adsorption technique has been widely used for the removal of asphaltenes and other heavy hydrocarbon species from crude oil using different types of sorbents,^{3,5} including the following: those available naturally, e.g., mineral surfaces such as clay,^{23,25–30} carbon,³¹ glass,^{32,33} silica,^{34,35} and reservoir rock;^{24,36} their components, such as quartz,³⁷ dolomite, calcite and kaolin,³⁸ soil³⁹ and mineral deposits;⁴⁰ metallic surfaces, such as gold,⁴¹ steel,⁴² and aluminum; and metal oxide surfaces such titanium and iron oxides.³⁸

In the adsorption processes, it is important to know the adsorbent surface chemistry and structure in terms of porosity and pore size.^{43,44} Typically, the adsorption processes of asphaltenes have been usually studied using nonporous material, which possess macropores or does not have pores that increase their external surface area. Moreover, experimental studies regarding asphaltene adsorption behavior have some limitations resulting from the complexity of asphaltene structures.^{45,46} The adsorption behaviors that exist in the presence of high asphaltene concentrations are complex and have not been adequately described analytically, although much has been learned about them.^{46,47} Asphaltenes could be adsorbed onto surfaces as molecules, nanoaggregates, micelles, dimers, and monomers. The source, concentration,^{35,48} and solvent strength of the solution⁴⁹ are important factors that could impact the degree of asphaltene association. Solvents such as benzene, toluene, xylenes, chloroform,⁵⁰ and CS₂⁵¹ are very good for asphaltenes dispersion, and depending on the concentration of the solution, the asphaltenes will be in different aggregate forms. For solutions at very low concentrations (>50–100 mg/L), the asphaltenes are present mainly as primary molecules or dimers,²² at relatively low concentration (100 mg/L up to 2000 and as high as 5000 mg/L) the asphaltenes are present in the form of nanoaggregates,²² and at higher concentrations (as low as 1500 mg/L but generally between 5000 and 50000 mg/L),^{52,53} the asphaltenes are present as associated clusters of nanoaggregates.²² However, it is important to know that these concentration ranges are not an absolute cutoff point in aggregation size. It has been

demonstrated that asphaltene adsorption from systems containing a precipitant agent such as *n*-pentane, *n*-hexane, or *n*-heptane increases the size of the asphaltene aggregate as the solubility parameter of the medium decreases,¹⁸ leading to bigger asphaltenes aggregates to be adsorbed,⁵⁴ generally in a “patchy” and heterogeneous way, as proven by atomic force microscopy (AFM).^{54–57} According to the findings by Zahabi et al.,⁵⁴ who used AFM to evaluate the heterogeneity of asphaltenes adsorbed on gold at different pentane/toluene ratios, as the asphaltenes aggregate increases, the steric repulsions are overcome and flocculation occurs because of driving forces resulting from the asphaltenes ability to stretch.^{22,47} The type and strength of the interactions between asphaltenes and surface sites are dependent on the functional groups and charge of the asphaltenes, as well as the chemistry and charge of the adsorbent surfaces.

Another important aspect about asphaltenes adsorption is that the adsorbent surface can drastically affect the way asphaltenes are adsorbed, guiding the asphaltenes layers reorganization over the adsorbent surface. This behavior has been reported by Dudášová et al.,⁵⁸ who studied crude oil asphaltenes adsorption onto hydrophobic silica (HS), kaolin, and FeS. For the kaolin and HS, the asphaltenes were adsorbed through the polar side of the molecule, leaving the nonpolar side free for the multilayer formation and is explained as the adsorption process is guided by steric stabilization, which means that the asphaltenes are adsorbed perpendicularly on the surface. On the other hand, for the FeS particles the asphaltenes could be adsorbed parallel to the surface, leaving both polar and nonpolar sides free for further adsorption and resulting in a lower uptake based on the adsorbent surface area.^{58,59} The type and strength of the interactions between asphaltenes and surface sites are dependent on the functional groups and charge of the asphaltenes and the chemistry of the adsorbent surfaces. Generally, asphaltene adsorption is studied in batch-mode processes to understand the adsorption kinetics and mechanism. Accordingly, two different types of adsorption isotherms have been reported in the literature, namely, Langmuir-type isotherms,⁶⁰ which indicate “effective” monolayer coverage of asphaltene on the solid surface^{22,25,30} and multisite and/or “effective” multilayer adsorption isotherms typically described by Freundlich model, which indicate aggregate formation and self-association of the asphaltene molecules as well as further formation of hemimicelles.^{22,28,35,38} However, because of the complex structure of asphaltenes with the ability to self-assemble into various aggregates and colloids, Langmuir and Freundlich models provide limited insight on the adsorption mechanism and behavior.

Alternatively, a molecular thermodynamics approach for modeling asphaltene adsorption isotherms was proposed by Castro et al.⁶¹ This model was successfully used to describe and correlate equilibrium asphaltene adsorption on rocks.⁶¹ However, the model requires the determination of 10 molecular parameters related to the size of the particles and the square-well potentials that describe particle–surface and particle–particle interactions in both bulk and adsorbed phases. Therefore, the practical use of this model is challenging and complicated. Recently, our research group⁶² has proposed the use of the Polanyi theory-based Dubinin–Ashtakhov (DA)⁶⁰ model for describing the adsorption of asphaltene onto surfaces of microparticles and nanoparticles. The proposed model requires the determination of three molecular parameters based on the energy of interactions between the surface and

adsorbate, the maximum adsorbed uptake, and the heterogeneity parameter. This model is extended for the first time to asphaltene adsorption onto different solid surfaces. In addition, our study showed that the isotherm experimental data of asphaltene adsorption fit better to the DA model than the commonly used Langmuir and Freundlich models.⁶² However, this DA model is not appropriate for describing the mechanism of adsorption of autoassociative molecules such as asphaltenes, especially at low loading and the consideration of the uniformly dense region at moderate loading.

Therefore, the present study employs, for the first time, a new model based on the “chemical theory”¹⁷ for describing the adsorption behavior of the autoassociative asphaltene molecules on different solid surfaces. The model is related to the equilibrium thermodynamic of sorption of asphaltenes onto solid surfaces taking into account the *i*-merization of the asphaltenes and its interaction with the surface at different temperatures have not been reported in the literature. The model is based on the chemical equilibria, the equation of state, and the phase equilibrium. The first two terms describe the behavior of the surface phase, and the phase equilibrium links the surface phase properties to bulk phase properties. Experimental data taken from published studies were used to determine the model's accuracy. Furthermore, the model was capable in determining the thermodynamic parameters of the adsorption process, such as ΔG° , ΔH° , and ΔS° .

2. THEORETICAL CONSIDERATIONS

Talu and Meunier proposed a thermodynamic model based on the general theory for the adsorption of associating molecules in micropores adsorbents.⁶³ The adsorption model, developed on the basis of “chemical theory”, is divided into three effective regimes for the adsorption of gas onto solid at different loading ranges, namely:

- (i) at low uptake, the behavior is described by adsorption of molecules on the high-energy sites, because of the preference and affinity of molecules in these sites for their strong interactions;⁶⁴
- (ii) at intermediate uptake, the adsorbate molecules form clusters via association around the high-energy sites via links by hydrogen bonding;⁶⁴ and
- (iii) at high uptake (typically the plateau region of the isotherm), the finite volume of adsorption becomes crowded with adsorbate molecules and, consequently, a limited amount of adsorption sites is available for adsorbate clusters.

In this study, for the first time, the chemical theory for describing the adsorption isotherms of complex molecules such as asphaltenes onto different solid surfaces has been proposed. Asphaltene adsorption from an oil medium (liquid phase) onto the particle surface is given by interactions between asphaltene–asphaltene and *i*-mers of asphaltene–solid surface. This behavior is due to the chemical nature of the asphaltene (i.e., autoassociative molecules). In the case of interactions of asphaltene–asphaltene molecules, the micelles formed as a result of quasi-chemical interactions between certain nonpolar compounds of hydrogen donors form (e.g., pyridine and aldehydes) and aromatic hydrocarbons (e.g., benzene).^{65,66} Asphaltene polar compounds have active hydrogen and, hence, the interaction cannot be of hydrogen bond types only. However, it appears to form a complex *i*-mer known as charge transfer complexes.⁶⁶ Accordingly, because of its amphiphilic

behavior and multifunctional character, asphaltene adsorption onto solid surfaces occurs, because of several intermolecular forces.^{67,68}

In addition, aggregate formation, self-association of the asphaltene molecules and further formation of hemimicelles on the solid surface during adsorption is likely to occur.⁶³ Here, we are employing the chemical theory for describing the adsorption behavior and self-association of asphaltene molecules on different solid surfaces.

2.1. Theory of Association on a Solid Surface. The physical and chemical theories of dissolution can predict and describe the behavior of solutions. For the case where the interaction forces are weak and there is no formation of new chemically stable species, the physical theory can be applied. Under the conditions where the interaction forces are strong (i.e., greater than the van der Waals forces), the chemical theory provides a reasonable description of the system (chemical solutions). This type of “chemical” solution is due to the nonideality given by the strong intermolecular forces present in the system.¹⁷ The chemical model explains dissolution properties from the interactions between molecules for generating new chemical species through its associations via hydrogen bonding or by the result of chemical reactions between them. These types of association reactions are linked to form the *i*-mer. The intensity of the bonds formed between the *i*-mers generally decrease with temperature and are favored with pressure. That is, the size of the polymer or the adsorbate clusters is affected by the increased temperature and favored by the increased pressure. It is expected that the *i*-mer is involved in sequential chain reactions to form the adsorbed clusters as follows:



where *b* is a monomer of the asphaltenes, which interacts with another monomer of the same family to form dimer, and the formed dimer interacts with a monomer forming a trimer and so forth. Subsequently, and depending on asphaltene concentration, asphaltenes in the form of monomer, dimer, trimer, etc. interact with the adsorbed phase on solid surface. The *i*-mer number formed depends on the conditions of pressure, concentration, temperature, and chemical structure of asphaltenes and solvent. The association rate constant is independent of the number of reactions (*i*). Furthermore, it is assumed that the molar and/or the volume of the polymer size is denoted by *i* multiplied by the number of independent cluster formation reactions (*i*) of the monomer. The number of independent reactions in the formation of the *i*-mer is more important than the reaction mechanism for equilibrium purposes, i.e., the formation of tetramer may be described on the interaction of two dimers or a trimer with a monomer, without any type of description of the thermodynamic equilibrium.

The proposed adsorption model is based on the cluster formation reactions on a solid surface. Therefore, an equilibrium state of an adsorbed phase is established when the minimum of total Gibbs free energy at constant temperature and spreading pressure (π) as described as follows:

$$d(nG)_{T,\pi} = 0 \quad (2)$$

Equation 2 can be expressed in terms of stoichiometric coefficients (v) and chemical potentials (μ) for each component involved in each independent reaction denoted by j :⁶⁵

$$d(nG)_{T,\pi} = \sum_i v_{ij} \mu_{ij} = 0 \quad (3)$$

when chemical equilibrium is achieved, the combinations in eq 3 are satisfied. Applying eq 3 for each reaction in eq 1, one can obtain^{17,65}

$$\mu_i = i \cdot \mu_1 \quad (4)$$

Equation 1 can be written in general form, if eq 4 is defined like a chemical reaction:^{17,65}

$$ib = b_i \quad (5)$$

Equation 5 describes that the product of i times a monomer (ib) is equal to i -mer (b_i).

2.2. Equation of State (EOS). In the “chemical theory”, the second step is to determine an equation of state (EOS) according to the considered system. Following the exact thermodynamic relations, the fugacity can be determined from an EOS as per eq 6:⁶⁵

$$RT \ln \frac{f_i}{x_i \pi} = \int_0^\pi \left[\left(\frac{\partial(n\bar{v}_i)}{\partial n_i} \right)_{T,\pi,n} - \frac{RT}{\pi} \right] d\pi \quad (6)$$

where \bar{v}_i is a partial molar volume.

Depending on the system complicity, π , v , and T behavior of a surface phase can be described from any EOS. For simplicity, the ideal-gas-like behavior in the surface phase could be considered. An ideal-gas EOS has two basic assumptions, namely (i) molecule has no volume (i.e., there is not cluster formation) and (ii) there are no lateral interactions between molecules.⁶⁸ This equation is too simplistic and, in this case, is unrealistic, especially for associating systems, because asphaltenes were large clusters that are likely to form. The second assumption is possible because the interaction between molecules can be neglecting in the Henry's law region. In this region, the vertical interactions are more important than lateral interactions due to the same phenomenology of adsorption process (at low adsorption uptake). However, for deviation from the ideality due to the cluster formation of asphaltenes, the behavior of fluid can be described by the EOS of Volmer,⁶⁹ which describes the real behavior and considers the volume occupied by the cluster size on the surface of adsorbent.

$$\pi(\bar{v} - b) = RT \quad (7)$$

Equation 7, the cluster size is subtracted from partial molar volume with the purpose of fulfilling condition (i). The b parameter is a volume correction factor that considers the volume occupied by the cluster size.

Substituting eq 7 in eq 6 and integrating gives the fugacity of a component with the Volmer EOS as

$$f_i = x_i \pi \exp\left(\frac{b_i \pi}{RT}\right) = x_i \pi \exp\left(\frac{ib_1 \pi}{RT}\right) \quad (8)$$

2.3. Phase Equilibrium. Now, it is worth noting that the modification of the model reported by Talu and Muenier⁶³

resides mainly in the phase equilibria, where we have used the equilibrium condition for the liquid and solid surface phases from the following expression:

$$\mu_i^L = \mu_i^S \Leftrightarrow \mu_1^L = \mu_1^S \quad (9)$$

At the same pressure and temperature, the chemistry potential for each component is equal in all phase equilibrium. Chemical potential of a liquid phase is defined as⁶⁵

$$\mu_i^L = \Gamma^L + RT \ln C \quad (10)$$

where, Γ^L is a phase liquid constant integration, which accounts for the reference state of the chemical potential (T, P), C is the concentration of monomers in the bulk phase. In a similar analogy, the solid phase chemical potential is given as

$$\mu_i^S = \Gamma^S + RT \ln f_i \quad (11)$$

Following the procedure proposed by the Talu and Meunier model,⁶³ but for liquid–solid equilibria, we have obtained our SLE equation as follows (details are provided in the Supporting Information).

$$C = \frac{\psi H}{1 + K\psi} \exp\left(\frac{\psi}{N_m}\right) \quad (12)$$

This adsorption isotherm model describes the behavior of asphaltenes onto a solid surface, i.e., solid–liquid equilibrium, which is a temperature-dependent model of three parameters (i.e., N_m , H , and K).^{6,70,71} H is the measured Henry's law constant, which is only a function of temperature, and an indicator of the adsorption affinity (i.e., the strength of interactions for adsorption) of asphaltenes onto solid surface. The lower the H value (i.e., higher Henry's constant), the higher the affinity (i.e., the active sites are in locations that are easily accessible by asphaltenes). K is constant and an indicator of rapid association of asphaltenes molecules once the primary sites are occupied. N_m is the maximum adsorption capacity of asphaltenes (g/g). The other parameters are defined as follows:

$$K = \frac{K_T RT}{SA} \quad (13)$$

$$\psi = \frac{-1 + \sqrt{1 + 4K\xi}}{2K} \quad (14)$$

where ξ is a constant (defined as $\xi = N_m N / (N_m - N)$), N is the amount adsorbed (g/g), K_T is the reaction constant for dimer formation, and SA is the specific surface area of the adsorbent.

To solve the model (eq 12), one needs to know the amount adsorbed (N , in g/g) and the equilibrium asphaltene concentration (C , in mg/g), both of which are measurable quantities of adsorption system that can be determined by the batch adsorption experiments. Then, through a nonlinear regression, it is possible to obtain the values of N_m , H , and K . In addition, the solid–liquid equilibrium (SLE) model can be used as a temperature-independent equation using five parameters, as it will be discussed in the upcoming sections. The model parameters are obtained by minimizing the error between theoretical C data and experimental data points using the DataFit software program (version 8.2.79, Oakdale Engineering, Oakdale, PA, USA). Accordingly, the error definition used was the root-mean-square error (RMS%) determined by eq 15. The calculated error values are tabulated. The RMS% was determined using the Microsoft Excel software package.

$$\text{RMS\%} = \sqrt{\frac{\sum_{i=1}^m (C_{\text{experimental},i} - C_{\text{model},i})^2}{m}} \times 100 \quad (15)$$

3. RESULTS AND DISCUSSION

The SLE model can help in understanding the different factors involved in the adsorption of asphaltenes. In this study, the SLE

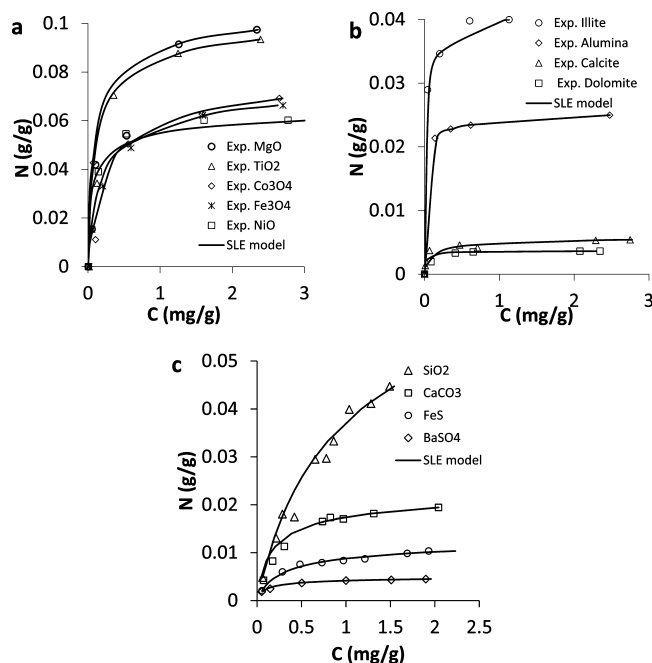


Figure 1. Isotherms of asphaltene adsorption onto different surfaces. The symbols are experimental data obtained from (a) Nassar et al.,⁷² (b) Dubey and Waxman,⁷¹ and (c) Dudášová et al.⁵⁹ The solid lines are from the solid–liquid equilibrium (SLE) model (see eq 12).

model results and analysis were divided into five sections, namely, (i) the effect of chemical nature of different surfaces of adsorbents, (ii) the chemical structure of asphaltenes used in the adsorption process, (iii) the effect of the temperature, (iv) thermodynamic studies, and (v) sensitivity analysis.

Table 2. Characteristics of the Considered Activated Carbon Prepared from Olive Stones

particle size (mm)	S_{BET} (m^2/g)	W_o (N_2) (cm^3/g)	W_o (CO_2) (cm^3/g)	L_o (N_2) (nm)	L_o (CO_2) (nm)	V_T (cm^3/g)
1.0–1.4	957	0.38	0.39	0.62	0.62	0.38

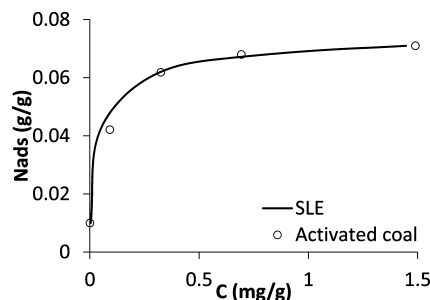


Figure 2. Isotherms of Colombian $n\text{C}_7$ -asphaltene adsorption onto activated carbon. The symbols represent the experimental data obtained, and the solid line is from the SLE model (eq 12).

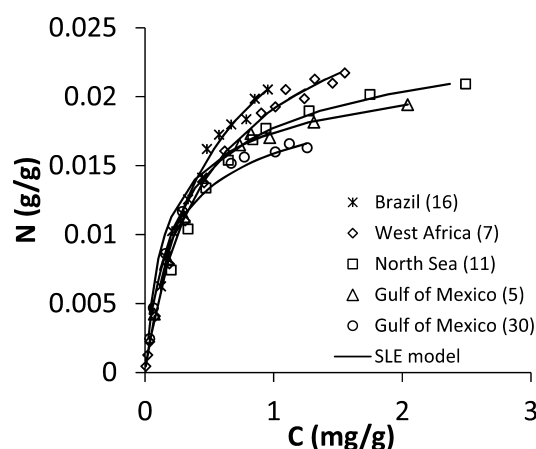


Figure 3. Isotherm adsorption of different types of asphaltenes onto CaCO_3 . The symbols represent experimental data obtained from Dudášová et al.,⁵⁹ and the solid lines are from the SLE model (eq 12).

Table 1. Estimated Parameters of SLE Model for Different Adsorbents

adsorbent	H [mg/g]	K [g/g]	N_m [g/g]	R^2	RMS%	ref
Co_3O_4	0.8959	0.00223	0.0973	0.99	8.82	Nassar et al. ⁷²
TiO_2	0.7093	0.00324	0.1328	0.99	4.37	Nassar et al. ⁷²
NiO	0.7138	0.00222	0.0809	0.99	3.20	Nassar et al. ⁷²
MgO	0.6371	0.00426	0.1377	0.99	5.62	Nassar et al. ⁷²
Fe_3O_4	2.0238	0.00330	0.1010	0.99	0.23	Nassar et al. ⁷²
dolomite	0.747	0.0003	0.0043	0.99	8.71	Dubey and Waxman ⁷¹
calcite	1.917	0.0001	0.0069	0.97	9.77	Dubey and Waxman ⁷¹
alumina	0.242	0.0004	0.0307	0.99	2.52	Dubey and Waxman ⁷¹
illite	0.272	0.0021	0.0524	0.99	9.74	Dubey and Waxman ⁷¹
FeS	20.72	0.0097	0.0175	0.98	5.37	Dudášová et al. ⁵⁹
BaSO_4	15.44	0.0021	0.0065	0.99	9.13	Dudášová et al. ⁵⁹
CaCO_3	6.316	0.0023	0.0303	0.98	6.91	Dudášová et al. ⁵⁹
SiO_2	11.52	0.0039	0.1172	0.97	5.18	Dudášová et al. ⁵⁹
activated carbon	0.2893	0.0021	0.0955	0.98	0.34	this study

Table 3. Estimated Parameters of the Solid–Liquid Equilibrium (SLE) Model for the Adsorption of Different Asphaltenes onto CaCO₃ Particles^a

asphaltene origin	<i>H</i> [g/g]	<i>K</i> [mg/g]	<i>N_m</i> [g/g]	<i>R</i> ²	RMS%
Gulf of Mexico (30)	8.753	0.0093	0.0292	0.97	3.5
North Sea (11)	9.406	0.0083	0.0344	0.99	9.2
West Africa (7)	14.869	0.0073	0.0458	0.98	6.5
Brazil (16)	14.198	0.0033	0.0511	0.97	3.3
Gulf of Mexico (5)	6.316	0.0023	0.0303	0.98	6.9

^aIn all cases, CaCO₃ was the adsorbent. Data taken from the work of Dudášová et al.⁵⁹

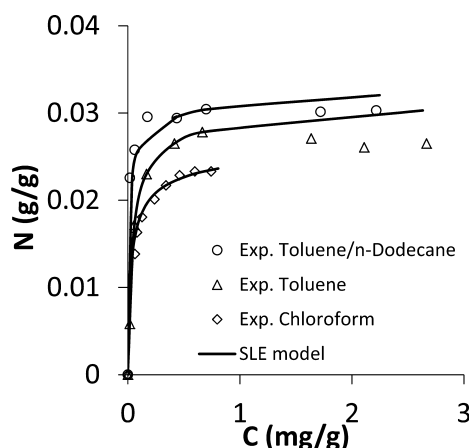


Figure 4. Isotherms adsorption of asphaltenes dissolved in different solvent onto kaolin. The symbols represent the experimental data obtained from Dubey and Waxman,⁷¹ and the solid lines are from the SLE model (eq 12).

Table 4. Estimated Parameters of SLE Model for Adsorption of Asphaltenes Dissolved in Different Solvents onto Kaolin^a

solvent	<i>H</i> [g/g]	<i>K</i> [mg/g]	<i>N_m</i> [g/g]	<i>R</i> ²	RMS%
chloroform	0.958	5.02	0.0297	0.99	4.5
toluene	0.043	5.08	0.0298	0.98	5.6
toluene– <i>n</i> -dodecane	0.040	5.36	0.0326	0.98	6.1

^aIn all cases, kaolin was the adsorbent. Data taken from the work of Dubey and Waxman.⁷¹

3.1. Effect of Chemical Nature of Adsorbent Surface.

Nassar et al.⁷² evaluated different metal oxide nanoparticles having different surface chemistry for adsorption of *n*C₇-asphaltenes from Athabasca vacuum residue. Dubey and Waxman⁷¹ tested different mineral surfaces that are likely present in rock structures for adsorptive removal of tar-sand derived *n*C₅-asphaltenes. Dudášová et al.⁵⁹ studied the adsorption of *n*C₅-asphaltenes from the Gulf of Mexico on different minerals and clays. Figures 1a, 1b and 1c show the experimental data obtained by Nassar et al.,⁷² Dubey and Waxman,⁷¹ and those obtained by Dudášová et al.,⁵⁹ respectively, together with the SLE model fits for adsorption of the corresponding asphaltenes. The values of the obtained model parameters and their corresponding RSM% values are presented in Table 1.

As seen in Figure 1 and Table 1, there is excellent agreement between the model and experimental results. Clearly, the RSM % values obtained for the experimental data reported by Nassar⁷² are lower than those reported by Dubey and Waxman.⁷¹ This could be attributed to the scatters in the

experimental data reported by Dubey and Waxman.⁷¹ Furthermore, as seen in Table 1, the SLE model parameters are adsorbent-specific. These differences in the values of SLE parameters could be attributed to the different degree of interaction between the asphaltene molecules or aggregates and the adsorbent surface.⁶² It is well-known that the adsorption of asphaltenes onto surfaces is dependent on the type and strength of interactions between the asphaltenes and the surface.⁷² For the case of minerals from Dubey and Waxman,⁷¹ as seen in Table 1, the illite and alumina showed the lowest values of the *H* parameter. This suggests that the surface of the mineral have a great affinity for the asphaltenes studied at Henry's law region, because of the high intermolecular forces between asphaltene molecules and the surface. This is not surprising, since illite contains iron in its structure,⁷³ which enhances the affinity toward asphaltenes. For the case of alumina, it is likely that the surface feature enhances polar interactions with the asphaltenes creating a higher affinity.^{59,72} These results are dependent on the chemical nature of asphaltene (i.e., polarity, aromaticity, content of heteroatoms, etc.) and the adsorbent surface chemistry. In addition, the results suggest that these minerals can change their wettability, which is supported by the lower values obtained for the *K* parameter. In the case of the SLE parameters for the adsorption isotherms obtained by Dudášová et al.,⁵⁹ the *N_m* values followed the order SiO₂ > FeS > CaCO₃ > BaSO₄, which is in excellent agreement with the order obtained by Dudášová et al.⁵⁹ As for the values of *H* and *K* parameters, results showed that CaCO₃ and SiO₂ have more affinity toward asphaltenes than the other adsorbents. According to the values of the *K* parameter, BaSO₄ and CaCO₃ lead to a lower degree of asphaltene self-association. For the case of oxide nanoparticles, as reported by Nassar et al.,⁷² the nanoparticles of Co₃O₄ and Fe₃O₄ have an amphoteric chemical structure, the nanoparticles of TiO₂ and NiO have an acidic chemical structure and MgO nanoparticles has a basic chemical structure. For metal oxide nanoparticles from the same group (i.e., Fe, Co, and Ni), the *H* values decreased in the following order: Fe₃O₄ > Co₃O₄ > NiO. This suggests that NiO nanoparticles have the highest affinity toward asphaltenes than the other oxides of the same group. This is in excellent agreement with the results reported by Nassar et al.⁷² However, comparing these nanoparticles with the other two oxides (i.e., MgO and TiO₂) the MgO nanoparticles have the lowest *H* value, suggesting a higher affinity. This indicates that the interactions between nanoparticles of oxides and asphaltenes are polar,⁷⁴ specifically acidic–basic.⁷² This is supported by the studies reported by Nassar et al.^{72,75,76} for the adsorption of Athabasca vacuum residue *n*C₇-asphaltenes, in the absence of water, onto different surfaces of metal oxides and alumina with different surface acidities. The authors found that the chemical nature of the adsorbent surface and the polarity, nitrogen content and the *H*/*C* ratio of the Athabasca vacuum residue *n*C₇-asphaltenes play roles in the adsorbent–adsorbate interactions. On the other hand, the order of the *K* values was as follows: Fe₃O₄ > Co₃O₄ ≈ NiO. This indicated that NiO and Co₃O₄ nanoparticles have a lower degree of asphaltene association on their surfaces than the Fe₃O₄ nanoparticles. This is in agreement with the results reported by Nassar et al.^{77,78} on the catalytic oxidation and thermal decomposition of the adsorbed asphaltenes onto different surfaces of oxides, where the authors showed that NiO and Co₃O₄ have comparable catalytic activity.

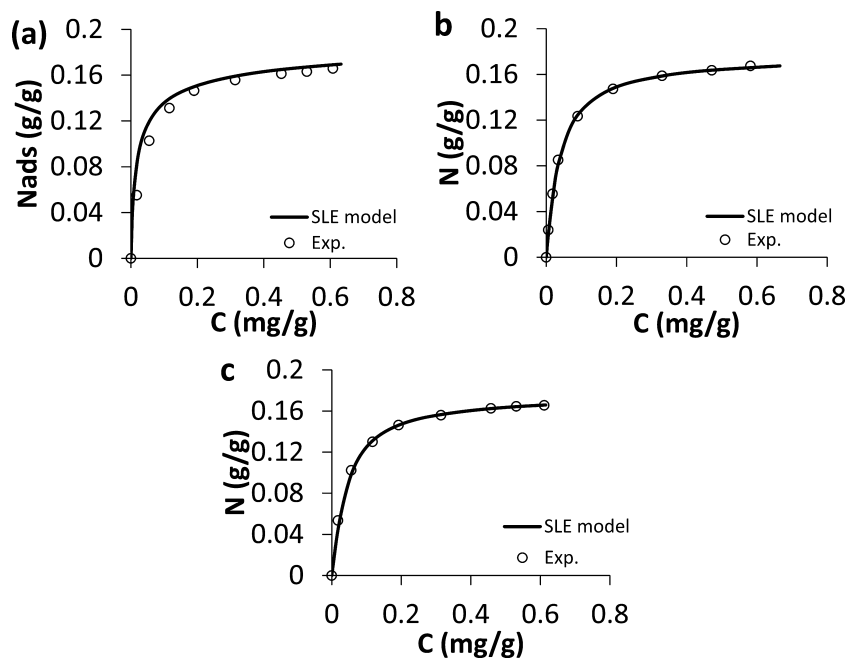


Figure 5. Isotherms of asphaltene adsorption onto AlNi15 nanoparticles at (a) 298 K, (b) 313 K, and (c) 328 K. The symbols represent experimental data obtained from Franco et al.,⁸⁸ and the solid lines are from the SLE model (eq 12).

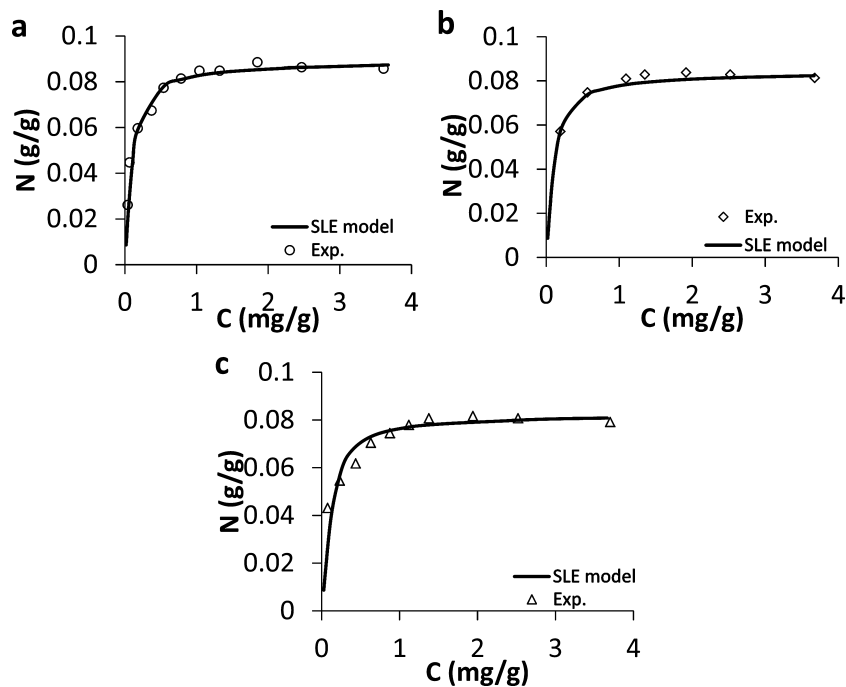


Figure 6. Isotherms of asphaltene adsorption onto γ -Al₂O₃ nanoparticles at (a) 298 K, (b) 313 K, and (c) 328 K. The symbols represent experimental data obtained from Nassar,⁴⁷ and the solid lines are from the SLE model (eq 12).

Table 5. Estimated Parameters of SLE Model at Different Temperatures

nanoparticle	temperature [K]	H [mg/g]	K [g/g]	N_m [g/g]	R^2	RMS%	ref
γ -Al ₂ O ₃	298	0.0992	0.0037	0.1069	0.99	6.62	Nassar ⁴⁷
γ -Al ₂ O ₃	313	0.1103	0.0038	0.1019	0.99	8.27	Nassar ⁴⁷
γ -Al ₂ O ₃	328	0.1394	0.0039	0.1011	0.99	8.09	Nassar ⁴⁷
AlNi15	298	0.0805	0.00324	0.2356	0.99	1.07	Franco et al. ⁸⁸
AlNi15	313	0.0855	0.00356	0.2344	0.99	1.05	Franco et al. ⁸⁸
AlNi15	328	0.0869	0.00357	0.2321	0.99	2.74	Franco et al. ⁸⁸

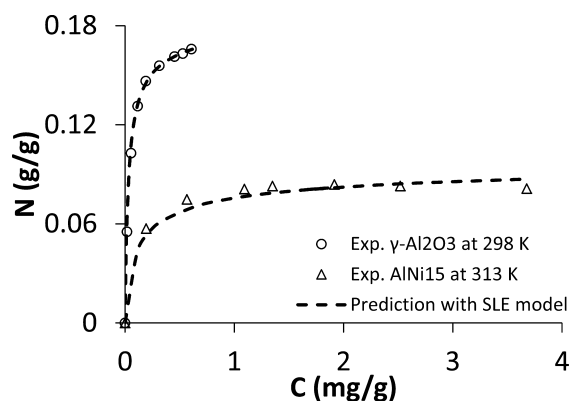


Figure 7. Isotherms of asphaltene adsorption onto AlNi15 at 298 K and γ -Al₂O₃ at 313 K. The symbols are experimental data obtained from Franco et al.⁸⁸ and Nassar,⁴⁷ respectively, and the dashed lines are prediction from SLE model of five parameters.

It should be noted here that the metal oxide nanoparticles reported by Nassar et al.⁷² are nonporous. For the materials reported by the other researchers (Dubey and Waxman⁷¹ and Dudášová et al.⁵⁹), the material porosity was not reported. Hence, to confirm the versatility of the proposed SLE model for both porous and nonporous materials, we evaluated the adsorption of Colombian *n*C₇-asphaltenes on in-house-prepared porous activated carbon (AC) originated from olive solid stones.⁷⁹ This sample was supplied by Dr. Carrasco-Marín from Universidad de Granada.⁷⁹ The surface area and porosity characterizations of the AC sample were performed by N₂ and CO₂ adsorption at −196 and 0 °C, respectively, using a conventional volumetric equipment made in Pyrex glass and free of mercury and grease, which reached a dynamic vacuum of more than 10^{−6} mbar at the sample location.⁷⁹ Equilibrium pressure was measured with a Baratron transducer from MKS. BET and the DR equation were applied to N₂ and CO₂ adsorption isotherms. Results of AC characterization are shown in Table 2, where *W*₀ and *L*₀ are micropore volume and micropore width accessible to these adsorptives (N₂ and CO₂), respectively. Based on N₂ adsorption isotherm obtained for the AC sample, a Type I behavior according to the IUPAC classification with a plateau practically parallel to the *p*/*p*₀-axis was demonstrated; this indicates that the considered AC is essentially microporous with none or very low mesoporosity.⁷⁹ Therefore, we can conclude that the material used in the experiment of *n*C₇-asphaltenes adsorption is porous material.

Figure 2 shows the obtained experimental data of adsorption isotherm of Colombian *n*C₇-asphaltenes on AC together with the SLE model fit. The values of the model parameters and their corresponding RSM% values are shown in Table 1. As seen, the obtained adsorption isotherm followed Type I behavior according to the IUPAC classification.⁸⁰ Furthermore, most importantly, excellent agreement between the SLE model and the experimental data is obtained, with a RSM% value of <1. This confirms that the proposed SLE model is capable of describing the adsorption isotherm on porous and nonporous surfaces.

Table 7. Estimated Thermodynamic Parameters for Asphaltene Adsorption onto γ -Al₂O₃ Nanoparticles from Nassar⁴⁷ and AlNi15 Nanoparticles from Franco et al.⁸⁸

adsorbent	temperature [K]	K	$-\Delta G_{\text{ads}}^{\circ}$ [kJ/mol]	$-\Delta H_{\text{ads}}^{\circ}$ [kJ/mol]	$-\Delta S_{\text{ads}}^{\circ}$ [J/(mol K)]
γ -Al ₂ O ₃	298	235.35	13.53		
	313	203.24	13.83	7.58	19.95
	328	177.88	14.13		
AlNi15	298	500.94	15.40		
	313	437.90	15.83	6.95	28.35
	328	387.53	16.25		

3.2. Effect of Chemical Structure of Asphaltenes and Its Dissolution in a Solvent. It is well-documented that the composition of asphaltenes is strongly dependent on the origin of crude oil and the method of extraction.^{81–85} Furthermore, the asphaltene chemical structure is also influenced by the solvent used for redissolution.⁷¹ In addition, the extent of aromaticity (i.e., low H/C ratio) and nitrogen content in the structure of asphaltenes can significantly impact asphaltene adsorption behavior,⁸⁵ as asphaltenes have a strong tendency to self-associate and, consequently, form aggregates.^{27,86} Therefore, understanding the chemical nature of asphaltenes and its behavior in different solvents, as well as the surface chemistry of the adsorbent, is of paramount importance for understanding the adsorption mechanism and behavior.^{9,27,39,81,87} Figure 3 shows the experimental data obtained by Dudášová et al.,⁵⁹ together with SLE model fits for adsorption isotherms of *n*C₅-asphaltenes of different origin onto CaCO₃ nanoparticles. The values of the obtained model parameters and their corresponding RSM% values are presented in Table 3. Clearly, the model parameters (i.e., *H*, *K*, and *N_m*) are dependent on the types of asphaltenes. Consequently, this reflects the specific interaction between CaCO₃ surfaces and the type of asphaltenes.⁵⁹ This is in excellent agreement with the observations reported by Dudášová et al.⁵⁹ on the Langmuir model parameters, where the variations of the *K_L* (that represents the affinity of interactions between the surface and asphaltene) and *Q_{max}* (which represents the maximum amount adsorbed due to the interaction and conformation of asphaltenes), as a function of the nature of the surface or asphaltenes, are different. It is worth noting here that the order of affinity ranking, represented by *H* values in our case, is different than those reported by Dudášová et al.⁵⁹ This could be due to the fact that Langmuir model does not reflect the degree of self-association of asphaltenes and also *K_L* depends more on the surface type than the structure of asphaltenes.⁵⁹ As seen, the degree of association or aggregation, represented by *K* values in our case, is dependent on the nature of asphaltenes. This shows that adsorption and the degree of interaction are not only dependent on the surface type, but also on the structure of asphaltenes and its degree of self-association and/or aggregation.

Furthermore, the amphiphilic behavior of the asphaltenes is related to the ratio of polar/nonpolar molecules present in their structure^{18,24,85} and the solvent used for extraction and

Table 6. Parameters of Five-Parameter SLE Model for Adsorption of Asphaltenes

adsorbent	<i>H</i> ₀	<i>H</i> ₁	<i>K</i> ₀	<i>K</i> ₁	<i>N_m</i> [g/g]	<i>R</i> ²	RMS%	ref
γ -Al ₂ O ₃	8.642	−2784.25	2.4	−912.2	0.1175	0.98	5.86	Nassar ⁴⁷
AlNi15	0.592	−709.66	3.41	−836.3	0.1980	0.99	1.46	Franco et al. ⁸⁸

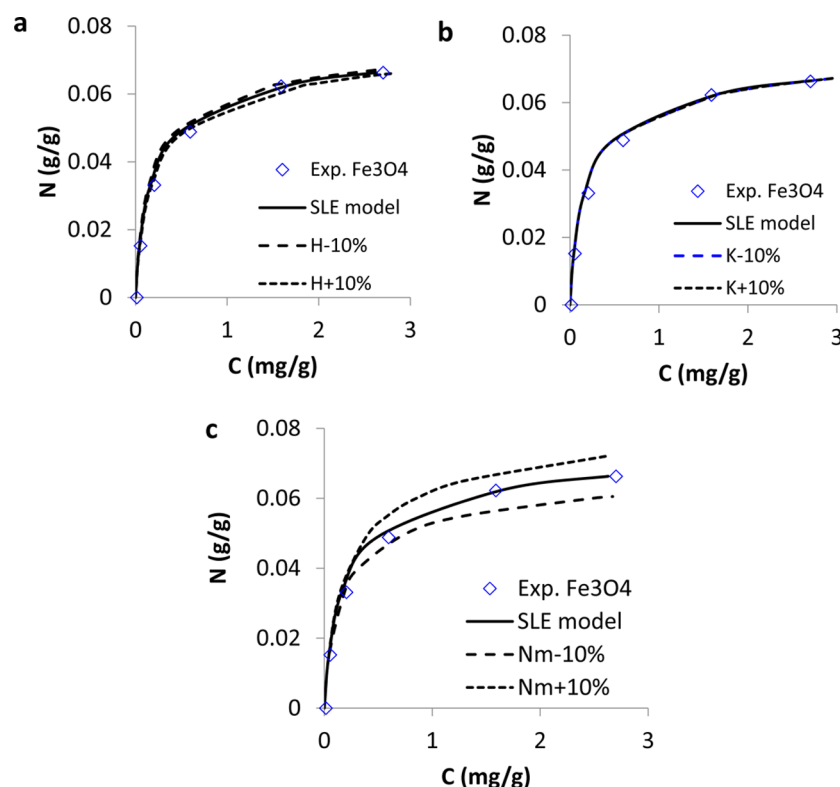


Figure 8. Sensitivity analysis of the three-parameter SLE model for the adsorption isotherm of Athabasca nC_7 -asphaltenes onto Fe_3O_4 nanoparticles ((a) H , (b) K , and (c) N_m). The symbols represent experimental data obtained from Nassar et al.,⁷² and the dashed lines represent the model prediction for a 10% increase or decrease in the model parameters.

dissolution,^{38,81,85} because, depending on that, the association will be better or worst. As the SLE model considers asphaltenes at the macroscopic level, the ratio of polar and nonpolar molecules present in the asphaltenes is not taken into account directly. Nevertheless, based on the values obtained for the K parameter, it can be explained whether asphaltene aggregation is favorable or unfavorable. In the case that the structure of the adsorbate do not have polar, nonpolar and functional groups with heteroatoms, the value of parameter K would be zero,⁶³ because the association between adsorbate molecules is unlikely to occur. Figure 4 shows the experimental data obtained by Dubey and Waxman⁷¹ for the adsorption of asphaltenes dissolved in different solvents (i.e., chloroform, toluene, and a 1.75:1 (w/w) mixture of toluene/ n -dodecane) onto kaolin, together with the SLE model fits. The values of the obtained model parameters and their corresponding RSM% values are presented in Table 4. As seen, the H values exhibited the following order: chloroform > toluene > toluene/ n -dodecane. Dubey and Waxman⁷¹ reported that the Hildebrand solubility parameters for chloroform, toluene, and toluene/ n -dodecane were 9.2, 8.9, and 8.7 $\text{cal}^{1/2} \text{cm}^{-3/2}$, respectively, indicating that the affinity of asphaltenes adsorption decreases as the solubility increases. The K -value for the toluene/ n -dodecane mixture was higher than that of toluene. This shows that the degree of interaction and self-association or aggregation of asphaltenes also is dependent on the type of solvent. The solubility of asphaltenes in the toluene/ n -dodecane mixture is less than that in toluene, allowing a greater preference for asphaltenes to be in the adsorbed phase than in the liquid phase (i.e., lower H).⁷¹ It should be noted here that the chloroform has a lower K -value than toluene and the toluene/ n -dodecane mixture, which

means that the degree of asphaltenes self-association in the adsorbent surface decreases as the solubility increases.

3.3. Effect of Temperature. Figures 5a–c show the experimental data obtained by Franco et al.,⁸⁸ together with SLE model fits for Colombian nC_7 -asphaltene adsorption onto nanoparticles of NiO supported on alumina support (AlNi15) at temperatures of 298 K (Figure 5a), 313 K (Figure 5b), and 328 K (Figure 5c). Similarly, Figures 6a–c show the experimental data obtained by Nassar,⁴⁷ together with SLE model fits for Athabasca bitumen nC_7 -asphaltene adsorption onto $\gamma\text{-Al}_2\text{O}_3$ nanoparticles at different temperatures. Worth noting here that, in both cases, the considered adsorbents were nonporous. As seen, all of the adsorption isotherms exhibited Type I behavior, according to the classification recommended by the International Union of Pure and Applied Chemistry (IUPAC).⁸⁰ Clearly, there is excellent agreement between the considered model and experimental results, as the RMS% values were <8.3%.

Table 5 shows the values of the model parameters for the aforementioned nanoparticles. Evidently, in both cases, the K and H parameters increased as the temperature increased. It is well-known that asphaltene adsorption is influenced by intermolecular forces between the asphaltene molecules and the solid surface.⁶² Asphaltenes can exhibit a wide variety of molecular structures, which results in more complex and varied aggregates (due to the various interactions that can occur).^{35,70,81,89,90} Accordingly, the temperature can have an impact on the aggregate behavior of asphaltenes and subsequently on the adsorption mechanism. This can be interpreted by looking into the trends of the values of K and H . The increase of H with the temperature suggests that the adsorption affinity between the solid surface and the

asphaltenes is decreasing. Therefore, when the temperature increases, the asphaltenes tend to remain mainly in the bulk phase instead of the solid surface, which is in agreement with the theory described by Prausnitz.¹⁷ Accordingly, in this case, the results suggest that the intermolecular forces between the surface of γ -Al₂O₃ nanoparticles and asphaltenes decreased with temperature. A similar conclusion can be drawn for the AlNi15 nanoparticles. However, AlNi15 showed lower H values in comparison with γ -Al₂O₃ nanoparticles at the same temperature. This indicates that the adsorption affinity is higher for the case of Colombian n C₇-asphaltenes. This is not surprising, since the presence of NiO on alumina would increase the surface acidity and subsequently enhance the affinity toward asphaltenes.⁷² This evidently proves that AlNi15 exhibits a synergistic effect, with regard to surface-active properties and functionality that lead to a better interaction with asphaltenes. Furthermore, as seen in Table 4, the trends for K values showed that it is increasing with the temperature, for both γ -Al₂O₃ and AlNi15 nanoparticles. This suggests that the extent of asphaltene self-association on the nanoparticle surface is increasing. Again, γ -Al₂O₃ nanoparticles showed higher K values than those of the AlNi15 nanoparticles at the same temperature. This suggests that the degree of asphaltene association and/or aggregation and cluster formation is higher for the γ -Al₂O₃ nanoparticles than the AlNi15 nanoparticles. This may be due to that the γ -Al₂O₃ nanoparticles have less active sites on the surface with affinity for the asphaltenes in comparison to AlNi15 nanoparticles. Hence, the presence of the NiO on the surface of the nanoparticles, as the NiO have high dispersion on the surface of alumina, would generate high affinity to the asphaltenes and subsequently inhibit cluster formation.⁸⁸ This is supported by the findings of Franco et al.,⁹¹ who studied the inhibition of formation damage due to asphaltene precipitation using different nanoparticles and found that NiO-supported alumina nanoparticles inhibited the asphaltene damage in porous media, because they eliminate the tendency to adsorb in multilayers, which could be due to remaining polarity of the initially adsorbed asphaltenes. Worth noting here that this comparison, between γ -Al₂O₃ and AlNi15, is not precise because the two asphaltenes are not of the same origin.

3.4. Five-Parameter SLE Model: Adsorption Isotherms Prediction and Thermodynamic Studies. The SLE model can be used to describe the adsorption at any temperature, using eqs 16 and 17 for H and K , respectively, with the isotherm expression (eq 12). The Henry's law constant is exponentially related to the inverse temperature and can be expressed as

$$H = \exp\left(H_0 + \frac{H_1}{T}\right) \quad (16)$$

Similarly, K can be expressed as

$$K = \exp\left(K_0 + \frac{K_1}{T}\right) \quad (17)$$

K_0 is related to reaction entropy and K_1 is related to reaction enthalpy of the dimer onto surface. In this case, only five temperature-independent parameters are necessary to describe the adsorption, namely, H_0 , H_1 , K_0 , K_1 , and N_m . Accordingly, the thermodynamic parameters of adsorption related to the association of the molecules of asphaltenes or in the cluster formation can be estimated.⁶³ Therefore, the change in

standard entropy ($\Delta S_{\text{ads}}^\circ$) and standard enthalpy ($\Delta H_{\text{ads}}^\circ$) can be estimated as follows:

$$\Delta S_{\text{ads}}^\circ = K_0 R \quad (18)$$

$$\Delta H_{\text{ads}}^\circ = K_1 R \quad (19)$$

The change in the standard Gibbs free energy is calculated according to the Gibbs equation:⁶⁵

$$\Delta G_{\text{ads}}^\circ = -RT \ln K \quad (20)$$

It is worth mentioning here that the five-parameter SLE model is also useful for predicting asphaltene adsorption isotherms at different temperatures. Therefore, the K_0 and K_1 parameters were estimated using the experimental data of the two adsorption isotherms at two different known temperatures for both AlNi15 and γ -Al₂O₃ nanoparticles. Then, the adsorption isotherms at the third temperature can be predicted. Figure 7 shows the experimental data of Colombian n C₇-asphaltenes adsorption isotherms onto AlNi15 at 298 K and Athabasca n C₇-asphaltenes adsorption isotherms onto γ -Al₂O₃ nanoparticles at 328 K, together with the five-parameter SLE prediction. Clearly, the model predicted the experimental data excellently, with the values obtained for R^2 and RSM% values of 0.99 and 3.3%, respectively, for AlNi15 nanoparticles and 0.98 and 7.8%, respectively, for γ -Al₂O₃ nanoparticles. Table 6 shows the results obtained by the five-parameter SLE model for the adsorption of asphaltenes onto γ -Al₂O₃ and AlNi15 previously mentioned.^{47,88} As seen, for the adsorption of asphaltenes onto γ -Al₂O₃, the value of K_1 is higher than the value obtained for AlNi15. Despite the fact that the asphaltenes and adsorbent used in both cases are different, if we make a comparison with the results obtained above with the three-parameter SLE model, the parameter K obtained for Nassar⁴⁷ was higher at all temperatures, with respect to the data reported by Franco et al.⁸⁸ The values obtained for the H parameter were also higher than the values obtained for the data of AlNi15, meaning that the adsorption onto γ -Al₂O₃ has a higher degree of asphaltenes self-association than that for asphaltene adsorption onto AlNi15. This is also supported by the thermodynamics parameters listed in Table 7. As seen, the results obtained for the association enthalpy on the surface phase (K_1) are adequate, because the system with γ -Al₂O₃ releases more heat than the system with AlNi15. Consequently, the estimated enthalpy changes for AlNi15 and γ -Al₂O₃ nanoparticles have values of 6.95 and 7.58 kJ/mol, respectively. It is worth noting here that Franco et al.⁸⁸ and Nassar⁴⁷ reported the $\Delta H_{\text{ads}}^\circ$ values based on the estimation of K values as the product between the equilibrium Langmuir constant (K_L) and the solvent molar concentration (C_s). The $\Delta H_{\text{ads}}^\circ$ values obtained by Franco et al.⁸⁸ and Nassar⁴⁷ were 3.07 and 3.90 kJ/mol, respectively, approximately half of the values obtained with the five-parameter SLE model. The difference between the values lies in that the $\Delta H_{\text{ads}}^\circ$ estimated using $K = K_L \times C_s$ assumes Type I monolayer adsorption of monomers on the adsorbent surface, resulting in underestimation of the change of reaction enthalpy. Instead, the $\Delta H_{\text{ads}}^\circ$ estimated through the five-parameter SLE model involves the asphaltene–asphaltene interaction for the dimer formation, leading to a higher change of association enthalpy. In the case of the change in entropy, the values calculated using the five-parameter SLE model are much lower than those obtained by Nassar⁴⁷ and Franco et al.⁸⁸ This, again, is because the SLE model accounts for asphaltene aggregation and cluster formation on the adsorbent surface. It is logical that

the values obtained with the Langmuir model are overestimated due that the randomness would be higher for *i*-mer adsorption than for dimer adsorption. Similar observations can be seen in the change of Gibbs free energy, where the values calculated by Nassar⁴⁷ and Franco et al.⁸⁸ are approximately twice those calculated through the five-parameter SLE model. Nevertheless, note that the negative values of $\Delta G_{\text{ads}}^{\circ}$ are an indication that asphaltene adsorption onto both AlNi15 and γ -Al₂O₃ nanoparticle surfaces is spontaneous and, hence, thermodynamically favorable. The negative values of $\Delta H_{\text{ads}}^{\circ}$ indicates that the interactions between the asphaltenes and the surfaces are exothermic. The positive values of $\Delta S_{\text{ads}}^{\circ}$ indicates an increase in the randomness at the solid/liquid interfaces. Note that this value is lower for the case of γ -Al₂O₃ nanoparticles than that of AlNi15, which supports the belief that there exists a higher degree of asphaltenes self-association onto γ -Al₂O₃ nanoparticles, which leads to cluster formation, than that in AlNi15 nanoparticles.

3.5. Sensitivity Analysis. To investigate the reliability of the three-parameter SLE model, a sensitivity analysis was performed. Figures 8a–c show the effect of a 10% increase or decrease in the values of the fitted SLE model parameters listed in Table 1 on the adsorption isotherms of Athabasca nC₇-asphaltenes onto Fe₃O₄ nanoparticles from Nassar et al.⁷² As seen, the N_m parameter is the most sensitive, while the K parameter is the lowest.

4. CONCLUSIONS

In this study, a solid–liquid equilibrium (SLE) model was developed based on the “chemical theory”, which accurately described the experimental data regarding different asphaltenes adsorption onto different solid surfaces (porous and non-porous) at different temperatures. In addition, the study found that the experimental data obtained for asphaltene adsorption fit very well to the SLE model with RSM% values lower than 10. In addition, we evaluated and validated the model where several authors used different solvents, types of asphaltenes and solid surfaces, which varying the formation of molecular aggregates, irregular packing and multilayer coverage the most common display of Type I behavior.

The proposed model was used for first time in this work to describe the adsorption of asphaltenes onto a surface based on the classic thermodynamics, where the *i*-mer formation of asphaltene, as a result of the interactions of asphaltene–asphaltene and asphaltene–surface, was included. In addition, the five-parameter SLE model is useful for adsorption isotherms prediction at different temperatures and to estimate the thermodynamic parameters employing the constant of dimer formation. The standard Gibbs free energy, enthalpy, and entropy changes of asphaltene adsorption onto adsorbent surfaces was successfully estimated. The sensitivity analysis revealed that the most sensitive parameter was N_m . This means that a slight variation of this parameter will result in considerable deviations between the experimental data and the model, whereas, with the K parameter, for the same variations, minimum deviation is observed. The preliminary results based on experimental data of several systems are very encouraging to further pursue the development of the association theory mainly at high pressure.

■ ASSOCIATED CONTENT

§ Supporting Information

This material is available free of charge via the Internet at <http://pubs.acs.org>.

■ AUTHOR INFORMATION

Corresponding Authors

*E-mail: nassar@ucalgary.ca (N. N. Nassar).

*E-mail: fbcortes@unal.edu.co (F. B. Cortes).

Notes

The authors declare no competing financial interest.

■ ACKNOWLEDGMENTS

The authors are grateful to Colciencias and Universidad Nacional de Colombia for logistical and financial support. The authors also acknowledge Dr. Pedro Pereira-Almao and Dr. Francis Meunier for fruitful discussions and assistance.

■ REFERENCES

- (1) Leontaritis, K. J. Asphaltene near-well-bore formation damage modeling. *J. Energy Resour. Technol.* **2005**, 127 (3), 191–200.
- (2) Speight, J. Petroleum Asphaltenes—Part 1: Asphaltenes, resins and the structure of petroleum. *Oil Gas Sci. Technol.* **2004**, 59 (5), 467–477.
- (3) Bockrath, B. C.; LaCount, R. B.; Noceti, R. P. *Fuel* **1980**, 59, 621.
- (4) Wargadalam, V. J.; Norinaga, K.; Iino, M. Size and shape of a coal asphaltene studied by viscosity and diffusion coefficient measurements. *Fuel* **2002**, 81 (11), 1403–1407.
- (5) Rosales, S.; Machín, I.; Sánchez, M.; Rivas, G.; Ruetter, F. *J. Mol. Catal. A: Chem.* **2006**, 246, 146.
- (6) Acevedo, S.; Castillo, J.; Fernández, A.; Goncalves, S.; Ranaudo, M. A. A study of multilayer adsorption of asphaltenes on glass surfaces by photothermal surface deformation. Relation of this adsorption to aggregate formation in solution. *Energy Fuels* **1998**, 12 (2), 386–390.
- (7) Mousavi-Dehghani, S.; Riazi, M.; Vafaie-Sefti, M.; Mansoori, G. An analysis of methods for determination of onsets of asphaltene phase separations. *J. Pet. Sci. Eng.* **2004**, 42 (2), 145–156.
- (8) Sheu, E. Y.; Shields, M. B.; Storm, D. A. Viscosity of base-treated asphaltene solutions. *Fuel* **1994**, 73 (11), 1766–1771.
- (9) Chianelli, R. R.; Siadati, M.; Mehta, A.; Pople, J.; Ortega, L. C.; Chiang, L. Y. Self-assembly of asphaltene aggregates: Synchrotron, simulation and chemical modeling techniques applied to problems in the structure and reactivity of asphaltenes. In *Asphaltenes, Heavy Oils, and Petroleomics*; Springer: New York, 2007; pp 375–400.
- (10) McLean, J. D.; Kilpatrick, P. K. Effects of asphaltene aggregation in model heptane–toluene mixtures on stability of water-in-oil emulsions. *J. Colloid Interface Sci.* **1997**, 196 (1), 23–34.
- (11) Acevedo, S.; Castro, A.; Negrin, J. G.; Fernández, A.; Escobar, G.; Piscitelli, V.; Delolme, F.; Dessalces, G. Relations between asphaltene structures and their physical and chemical properties: The rosary-type structure. *Energy Fuels* **2007**, 21 (4), 2165–2175.
- (12) Groenzin, H.; Mullins, O. C. *J. Phys. Chem. A* **1999**, 103, 11237.
- (13) Mullins, O. C. The asphaltenes. *Ann. Rev. Anal. Chem.* **2011**, 4, 393–418.
- (14) Mullins, O. C.; Sabbah, H.; Eyssautier, J. I.; Pomerantz, A. E.; Barré, L.; Andrews, A. B.; Ruiz-Morales, Y.; Mostowfi, F.; McFarlane, R.; Goual, L. Advances in asphaltene science and the Yen–Mullins model. *Energy Fuels* **2012**, 26 (7), 3986–4003.
- (15) Lopez-Linares, F.; Carbognani, L.; Hassan, A.; Pereira-Almao, P.; Rogel, E.; Ovalles, C.; Pradhan, A.; Zintsmaster, J. Adsorption of Athabasca vacuum residues and their visbroken products over macroporous solids: influence of their molecular characteristics. *Energy Fuels* **2011**, 25 (9), 4049–4054.
- (16) Spiecker, P. M.; Gawrys, K. L.; Trail, C. B.; Kilpatrick, P. K. Effects of petroleum resins on asphaltene aggregation and water-in-oil emulsion formation. *Colloids Surf. A* **2003**, 220 (1), 9–27.

- (17) Prausnitz, J. M.; Lichtenthaler, R. N.; de Azevedo, E. G. *Molecular Thermodynamics of Fluid-Phase Equilibria*; Pearson Education: Upper Saddle River, NJ, 1998.
- (18) Spiecker, P. M.; Gawrys, K. L.; Kilpatrick, P. K. Aggregation and solubility behavior of asphaltenes and their subfractions. *J. Colloid Interface Sci.* **2003**, 267 (1), 178–193.
- (19) Witthayapanyanon, A.; Harwell, J.; Sabatini, D. Hydrophilic–lipophilic deviation (HLD) method for characterizing conventional and extended surfactants. *J. Colloid Interface Sci.* **2008**, 325 (1), 259–266.
- (20) Mittal, K. L.; Shah, D. O. *Adsorption and Aggregation of Surfactants in Solution*. Marcel Dekker: New York, 2002.
- (21) Mullins, O. C.; Sheu, E. Y. *Structures and Dynamics of Asphaltenes*. Plenum Press: New York, 1999.
- (22) Adams, J. J. Asphaltene Adsorption: A Literature Review. *Energy Fuels* **2014**, 28 (5), 2831–2856.
- (23) Pernyeszi, T.; Dékány, I. Sorption and elution of asphaltenes from porous silica surfaces. *Colloids Surf., A* **2001**, 194 (1–3), 25–39.
- (24) Pernyeszi, T.; Patzkó, Á.; Berkesi, O.; Dékány, I. Asphaltene adsorption on clays and crude oil reservoir rocks. *Colloids Surf., A* **1998**, 137 (1–3), 373–384.
- (25) Marlow, B.; Sresty, G.; Hughes, R.; Mahajan, O. Colloidal stabilization of clays by asphaltenes in hydrocarbon media. *Colloids Surf.* **1987**, 24 (4), 283–297.
- (26) Menon, V. B.; Wasan, D. T. *Colloids Surf.* **1987**, 23, 353.
- (27) Saada, A.; Siffert, B.; Papirer, E. Comparison of the hydrophilicity/hydrophobicity of illites and kaolinites. *J. Colloid Interface Sci.* **1995**, 174 (1), 185–190.
- (28) González, G.; Moreira, M. B. The wettability of mineral surfaces containing adsorbed asphaltene. *Colloids Surf.* **1991**, 58 (3), 293–302.
- (29) Bantignies, J. L.; Cartier dit Moulin, C.; Dexpert, H. *J. Pet. Sci. Eng.* **1998**, 20, 233.
- (30) Gaboriau, H.; Saada, A. Influence of heavy organic pollutants of anthropic origin on PAH retention by kaolinite. *Chemosphere* **2001**, 44 (7), 1633–1639.
- (31) Sakanishi, K.; Saito, I.; Watanabe, I.; Mochida, I. *Fuel* **2004**, 83, 1889.
- (32) Akhlag, M. S.; Götze, P.; Kessel, D.; Dornow, W. *Colloids Surf., A* **1997**, 126, 25.
- (33) Castillo, J.; Goncalves, S.; Fernández, A.; Mujica, V. *Opt. Commun.* **1998**, 145, 69.
- (34) Kumar, K.; Dao, E.; Mohanty, K. J. *J. Colloid Interface Sci.* **2005**, 289, 206.
- (35) Acevedo, S.; Ranaudo, M.; García, C.; Castillo, J.; Fernández, A.; Caetano, M.; Goncalves, S. *Colloids Surf., A* **2000**, 166, 145.
- (36) Alkafef, S. F.; Algharaib, M. K.; Alajmi, A. F. *J. Colloid Interface Sci.* **2006**, 298, 13.
- (37) González, G.; Middea, A. *Colloids Surf.* **1991**, 52, 207.
- (38) Marczewski, A. W.; Szymula, M. Adsorption of asphaltenes from toluene on mineral surface. *Colloids Surf., A* **2002**, 208 (1), 259–266.
- (39) Szymula, M.; Marczewski, A. W. Adsorption of asphaltenes from toluene on typical soils of Lublin region. *Appl. Surf. Sci.* **2002**, 196 (1), 301–311.
- (40) Cosultchi, A.; Garciafigueroa, E.; Mar, B.; García-Bórquez, A.; Lara, V. H.; Bosch, P. *Fuel* **2002**, 81, 413.
- (41) Ekholm, P.; Blomberg, E.; Claesson, P.; Auflem, I. H.; Sjöblom, J.; Kornfeldt, A. *J. Colloid Interface Sci.* **2002**, 247, 342.
- (42) Abdallah, W.; Taylor, S. Surface characterization of adsorbed asphaltene on a stainless steel surface. *Nucl. Instrum. Methods Phys. Res., Sect. B* **2007**, 258 (1), 213–217.
- (43) Hassan, A.; Lopez-Linares, F.; Nassar, N. N.; Carbognani-Arambarri, L.; Pereira-Almao, P. Development of a support for a NiO catalyst for selective adsorption and post-adsorption catalytic steam gasification of thermally converted asphaltenes. *Catal. Today* **2013**, 207, 112–118.
- (44) Thommes, M. Physical adsorption characterization of nanoporous materials. *Chem. Ing. Techn.* **2010**, 82 (7), 1059–1073.
- (45) Mendoza de la Cruz, J. L.; Castellanos-Ramírez, I. V.; Ortiz-Tapia, A.; Buenrostro-González, E.; Durán-Valencia, C. d. I. A.; López-Ramírez, S. Study of monolayer to multilayer adsorption of asphaltenes on reservoir rock minerals. *Colloids Surf., A* **2009**, 340 (1), 149–154.
- (46) Marczewski, A.; Szymula, M. Adsorption of asphaltenes from toluene on quartz and silica-rich soils. *Adsorption* **2003**, 58, (4).
- (47) Nassar, N. N. Asphaltene Adsorption onto Alumina Nanoparticles: Kinetics and Thermodynamic Studies. *Energy Fuels* **2010**, 24 (8), 4116–4122.
- (48) Mostowfi, F.; Indo, K.; Mullins, O. C.; McFarlane, R. Asphaltene Nanoaggregates Studied by Centrifugation†. *Energy Fuels* **2008**, 23 (3), 1194–1200.
- (49) Simon, S.; Jestin, J.; Palermo, T.; Barré, L. C. Relation between solution and interfacial properties of asphaltene aggregates. *Energy Fuels* **2008**, 23 (1), 306–313.
- (50) Clementz, D. M. Interaction of petroleum heavy ends with montmorillonite. *Clays Clay Miner.* **1976**, 24 (6), 312–319.
- (51) Fritschy, G.; Papirer, E. Interactions between a bitumen, its components and model fillers. *Fuel* **1978**, 57 (11), 701–704.
- (52) Andersen, S. I. Association of Petroleum Asphaltenes and the Effect on Solution Properties. In *Handbook of Surface and Colloid Chemistry*, 3rd Edition; Birdi, K. S., Ed.; CRC Press/Taylor and Francis: Boca Raton, FL, 2009; Chapter 18, p 703.
- (53) Mullins, O. C.; Seifert, D. J.; Zuo, J. Y.; Zeybek, M. Clusters of asphaltene nanoaggregates observed in oilfield reservoirs. *Energy Fuels* **2012**, 27 (4), 1752–1761.
- (54) Zahabi, A.; Gray, M. R.; Dabros, T. Heterogeneity of Asphaltene Deposits on Gold Surfaces in Organic Phase Using Atomic Force Microscopy. *Energy Fuels* **2012**, 26 (5), 2891–2898.
- (55) Toulhoat, H.; Prayer, C.; Rouquet, G. Characterization by atomic force microscopy of adsorbed asphaltenes. *Colloids Surf., A* **1994**, 91, 267–283.
- (56) Tu, Y.; Kingston, D.; Kung, J.; Kotlyar, L. S.; Sparks, B. D.; Chung, K. H. Adsorption of pentane insoluble organic matter from oilsands bitumen onto clay surfaces. *Pet. Sci. Technol.* **2006**, 24 (3–4), 327–338.
- (57) Balabin, R. M.; Syunyaev, R. Z.; Schmid, T.; Stadler, J.; Lomakina, E. I.; Zenobi, R. Asphaltene adsorption onto an iron surface: combined near-infrared (NIR), Raman, and AFM study of the kinetics, thermodynamics, and layer structure. *Energy Fuels* **2010**, 25 (1), 189–196.
- (58) Dudášová, D.; Flåten, G. R.; Sjöblom, J.; Øye, G. Study of asphaltenes adsorption onto different minerals and clays: Part 2. Particle characterization and suspension stability. *Colloids Surf., A* **2009**, 335 (1), 62–72.
- (59) Dudášová, D.; Simon, S.; Hemmingsen, P. V.; Sjöblom, J. Study of asphaltenes adsorption onto different minerals and clays: Part 1. Experimental adsorption with UV depletion detection. *Colloids Surf., A* **2008**, 317 (1), 1–9.
- (60) Lowell, S.; Shields, J. E. *Powder Surface Area and Porosity*; Chapman and Hall: London, 1991; Vol. 2.
- (61) Castro, M.; de la Cruz, J. L. M.; Buenrostro-Gonzalez, E.; López-Ramírez, S.; Gil-Villegas, A. Predicting adsorption isotherms of asphaltenes in porous materials. *Fluid Phase Equilib.* **2009**, 286 (2), 113–119.
- (62) Giraldo, J.; Nassar, N. N.; Benjumea, P.; Pereira-Almao, P.; Cortés, F. B. Modeling and Prediction of Asphaltene Adsorption Isotherms Using Polanyi's Modified Theory. *Energy Fuels* **2013**, 27 (6), 2908–2914.
- (63) Talu, O.; Meunier, F. Adsorption of associating molecules in micropores and application to water on carbon. *AIChE J.* **1996**, 42 (3), 809–819.
- (64) Dubinin, M. Water vapor adsorption and the microporous structures of carbonaceous adsorbents. *Carbon* **1980**, 18 (5), 355–364.
- (65) Smith, J. M.; Van Ness, H. C.; Abbott, M. M. *Introduction to Chemical Engineering Thermodynamics*; McGraw-Hill: New York, 2005.
- (66) Henri, R.; Prausnitz, J. On the thermodynamics of alcohol–hydrocarbon solutions. *Chem. Eng. Sci.* **1967**, 22 (3), 299–307.

- (67) Florry, P. Thermodynamics of heterogeneous Polymers and Their Solutions. *J. Chem. Phys.* **1944**, *12*, 425.
- (68) Dolezalek, F. Zur Theorie der binären Gemische und konzentrierten Lösungen. *Z. Phys. Chem.* **1908**, *64*, 727–747.
- (69) Mulliken, R. S.; Person, W. B. *Molecular Complexes: A Lecture and Reprint Volume*; Wiley–Interscience: New York, 1969.
- (70) Fenistein, D.; Barré, L.; Broseta, D.; Espinat, D.; Livet, A.; Roux, J.-N.; Scarsella, M. Viscosimetric and neutron scattering study of asphaltene aggregates in mixed toluene/heptane solvents. *Langmuir* **1998**, *14* (5), 1013–1020.
- (71) Dubey, S.; Waxman, M. Asphaltene adsorption and desorption from mineral surfaces. *SPE Reservoir Eng.* **1991**, *6* (03), 389–395.
- (72) Nassar, N. N.; Hassan, A.; Pereira-Almao, P. Metal oxide nanoparticles for asphaltene adsorption and oxidation. *Energy Fuels* **2011**, *25* (3), 1017–1023.
- (73) Manning, B. A.; Goldberg, S. Modeling arsenate competitive adsorption on kaolinite, montmorillonite and Illite. *Clays Clay Miner.* **1996**, *44* (5), 609–623.
- (74) Cortés, F. B.; Mejía, J. M.; Ruiz, M. A.; Benjumea, P.; Riffel, D. B. Sorption of Asphaltenes onto Nanoparticles of Nickel Oxide Supported on Nanoparticulated Silica Gel. *Energy Fuels* **2012**, *26* (3), 1725–1730.
- (75) Nassar, N. N.; Hassan, A.; Carbognani, L.; Lopez-Linares, F.; Pereira-Almao, P. Iron oxide nanoparticles for rapid adsorption and enhanced catalytic oxidation of thermally cracked asphaltenes. *Fuel* **2012**, *95*, 257–262.
- (76) Nassar, N. N.; Hassan, A.; Pereira-Almao, P. Effect of surface acidity and basicity of aluminas on asphaltene adsorption and oxidation. *J. Colloid Interface Sci.* **2011**, *360*, 233–238.
- (77) Nassar, N.; Hassan, A.; Pereira-Almao, P. Thermogravimetric studies on catalytic effect of metal oxide nanoparticles on asphaltene pyrolysis under inert conditions. *J. Therm. Anal. Calorim.* **2012**, *110* (3), 1327–1332.
- (78) Nassar, N. N.; Hassan, A.; Pereira-Almao, P. Comparative oxidation of adsorbed asphaltenes onto transition metal oxide nanoparticles. *Colloids Surf., A* **2011**, *384* (1–3), 145–149.
- (79) Ubago-Pérez, R.; Carrasco-Marín, F.; Fairén-Jiménez, D.; Moreno-Castilla, C. Granular and monolithic activated carbons from KOH-activation of olive stones. *Microporous Mesoporous Mater.* **2006**, *92* (1), 64–70.
- (80) Sing, K.; Sing, K.; Everett, D.; Haul, R.; Moscou, L.; Pierotti, R.; Rouquerol, J.; Siemieniowska, T. Reporting physisorption data for gas/solid systems. *Pure Appl. Chem.* **1982**, *54* (11), 2201.
- (81) Groenzin, H.; Mullins, O. C. Molecular Size and Structure of Asphaltenes from Various Sources. *Energy Fuels* **2000**, *14* (3), 677–684.
- (82) McLean, J. D.; Kilpatrick, P. K. Effects of asphaltene solvency on stability of water-in-crude-oil emulsions. *J. Colloid Interface Sci.* **1997**, *189* (2), 242–253.
- (83) Sharma, M. K.; Yen, T. F. *Asphaltene Particles in Fossil Fuel Exploration, Recovery, Refining, and Production Processes*; Plenum Press: New York, 1994.
- (84) Peng, P. a.; Fu, J.; Sheng, G.; Morales-Izquierdo, A.; Lown, E. M.; Strausz, O. P. Ruthenium-ions-catalyzed oxidation of an immature asphaltene: Structural features and biomarker distribution. *Energy Fuels* **1999**, *13* (2), 266–277.
- (85) López-Linares, F.; Carbognani, L.; Sosa-Stull, C.; Pereira-Almao, P.; Spencer, R. J. Adsorption of virgin and visbroken residue asphaltenes over solid surfaces. 1. Kaolin, smectite clay minerals, and athabasca siltstone. *Energy Fuels* **2009**, *23* (4), 1901–1908.
- (86) Goncalves, S.; Castillo, J.; Fernandez, A.; Hung, J. Absorbance and fluorescence spectroscopy on the aggregation behavior of asphaltene–toluene solutions. *Fuel* **2004**, *83* (13), 1823–1828.
- (87) Carlos da Silva Ramos, A.; Haraguchi, L.; Notrispe, F. R.; Loh, W.; Mohamed, R. S. Interfacial and colloidal behavior of asphaltenes obtained from Brazilian crude oils. *J. Pet. Sci. Eng.* **2001**, *32* (2), 201–216.
- (88) Franco, C.; Patiño, E.; Benjumea, P.; Ruiz, M. A.; Cortés, F. B. Kinetic and thermodynamic equilibrium of asphaltenes sorption onto nanoparticles of nickel oxide supported on nanoparticulated alumina. *Fuel* **2013**, *105* (0), 408–414.
- (89) Browarzik, D.; Laux, H.; Rahimian, I. Asphaltene flocculation in crude oil systems. *Fluid Phase Equilib.* **1999**, *154* (2), 285–300.
- (90) Sanders, R.; Chow, R.; Masliyah, J. Deposition of bitumen and asphaltene-stabilized emulsions in an impinging jet cell. *J. Colloid Interface Sci.* **1995**, *174* (1), 230–245.
- (91) Franco, C. A.; Nassar, N. N.; Ruiz, M. A.; Pereira-Almao, P.; Cortés, F. B. Nanoparticles for Inhibition of Asphaltenes Damage: Adsorption Study and Displacement Test on Porous Media. *Energy Fuels* **2013**, *27* (6), 2899–2907.